

Amplified Msf tides at Kochi backwaters on the southwest coast of India

Antony Joseph^{1,*}, K. K. Balachandran², Prakash Mehra¹, R. G. Prabhudesai¹, Vijay Kumar¹, Yogesh Agarvadekar¹, C. Revichandran² and Nitin Dabholkar¹

¹National Institute of Oceanography (CSIR), Dona Paula, Goa 403 004, India

²National Institute of Oceanography (CSIR), Regional Centre, Dr Salim Ali Road, Kochi 682 018, India

Characteristics of tides at eight stations in Kochi backwaters (KB) located on the southwest coast of India are analysed. The Msf tidal constituents at several locations are found to be considerably larger than those estimated from the driving tidal potential. The Msf tidal amplitude amplifies progressively from Kochi inlet to the shallower upstream region where it exhibits ~3-fold amplification. At the upstream boundary, the Msf tide has the same order of magnitude as M_2 and K_1 tides. The nonlinear frictional interaction between M_2 and S_2 tides appears to be mainly responsible for the observed amplification. However, in regions where depth is <2 m, variable bottom frictional effects at fortnightly periodicity plays an additional role in the Msf tidal amplification.

Keywords: Amplification, bed materials, Kochi backwaters, nonlinear frictional interaction, shallowness, tides.

NOTICEABLE transformations occur in the pattern and range of tides during their propagation from the open ocean into continental shelves and further into shallower coastal waters, broad lagoons and backwaters. Such transformations, caused by a myriad of topographical and bathymetric influences, are indicated by the presence of relatively large-amplitude over-tides and compound-tides. These tidal constituents represent the nonlinear harmonics generated primarily under the influence of large bottom friction. Wave phenomena such as reflection, resonance, etc. may also affect the various tidal constituents in different ways. Mutual interaction of the tidal constituents exerts an important influence on the propagation and shape of the tides in estuaries and backwaters. The study presented in this article reports the characteristics of tides at Kochi backwater (KB) system on the southwest coast of India based on *in situ* time-series tidal measurement results. The present tidal measurements from eight stations covering the entire KB indicate that the upstream boundary regions of KB and its inter-mouth region exhibit prominent fortnightly tidal character because of the presence of Msf tidal constituent (14.76 day period)

whose amplitude is relatively larger than what is generally found. The theme of this article is primarily about the large Msf tides observed at a few stations in KB, which is a new finding in these areas.

Large Msf tidal constituent has been reported from relatively fewer sites in the world. In the Pacific Ocean, Msf tide has been identified at Canton Island¹. In the Atlantic Ocean, alongshore propagating large Msf tide has been observed at a few locations along the northern coast of the Gulf of Guinea². This constituent has also been identified in St Lawrence estuary, Canada³, several locations of an English tidal lagoon known as the Fleet⁴, and the Amazon estuary in North America⁵. Except for the Msf tides of amplitudes up to ~5 cm in the upstream regions of Mandovi and Zuari estuaries in Goa⁶, information on Msf tides in the Indian Ocean is lacking. It was reported that the Msf tide has considerable impact on the water level regime and salinity distribution in the Fleet lagoon, and forces strong vertical oscillations of the sub-surface thermal structure in the Guinea Gulf.

Although the Msf tidal motions are relatively weak (~1 cm at most coastal locations)⁷, they are considered to be important in modern oceanography because of their influence on the more general motions existing in the ocean at low frequencies⁸. In the present study, we analyse the time-series data of tidal measurements from eight stations covering the entire KB, for durations exceeding a month (Table 1) to examine the characteristics of tides in these locations and to understand the observed large Msf tidal constituent at the inter-mouths and the upstream regions of KB.

Description of study areas

The KB system, from which *in situ* tidal measurements have been made, is a shallow semi-enclosed water body (average depth = 2.5 m) having multiple branches, ~82 km in length and ~256 km² in area, trapped behind and running parallel to the southwest coast of India. This water body, characterized by irregular topography and interspersed by numerous islets and shoals of varied sizes and shapes, is the largest and the most complex estuarine system on the west coast of India. A shallow region

*For correspondence. (e-mail: joseph@nio.org)

Table 1. Summary of sea-level measurement locations and durations of time-series measurements. Station numbers provided against the station names correspond to those indicated in the location map in Figure 1. Tide measurements from Kochi backwaters (stations 1–8 in Figure 1) were made using float-driven gauges, in which station #2 used a conventional Survey of India paper chart gauge. Stations #1, and #3–8 used EMCON-make electronic gauges

Station number and name	Latitude	Longitude	Measurement duration
(1) Nedumgad	10°04.37'N	76°13.66'E	20 April–4 June 2006
(2) Cochi Port Trust	09°58.34'N	76°14.60'E	26 April–6 June 2006
(3) Vytilla	09°57.17'N	76°18.89'E	12 April–19 May 2006
(4) Vaduthala	09°51.41'N	76°20.34'E	11 April–3 June 2006
(5) Vettikattumukku	09°48.58'N	76°27.26'E	11 April–27 May 2006
(6) Vayalar	09°42.69'N	76°20.63'E	23 April–3 June 2006
(7) Thaneermukkam	09°40.82'N	76°23.37'E	23 April–3 June 2006
(8) Talavadi	09°31.77'N	76°21.27'E	27 April–3 June 2006

(average depth ~2 m) of ~70 km² in area, known as Vembanad Lake, which is situated at the southern end of the estuary is the broadest segment of KB. The dual mouths of KB (one at Azhikode (250 m wide) and another at Kochi (450 m wide) which are separated by ~25 km), which open to the eastern Arabian Sea allow tidal propagation in this estuary. Figure 1 shows the measurement locations, and indicates the topography and bathymetry of KB.

Sparsity of tidal measurements in the study areas

Although tides in KB have been examined in the past based on measurements of very short duration from a few locations, such measurements are largely limited to the vicinity of the Kochi inlet⁹. For a subsequent study, tidal measurements have been obtained in October 2003 from seven stations covering Cochin Port Trust to Thanneermukkom hydraulic barrage in the southern segment of the estuary. However, measurements from six of these stations are limited to day time, from 6 am to 6 pm, and therefore computed tides obtained from a 2D hydrodynamic model had to be relied upon for studies related to tidal circulation, pollutant dispersion, etc.¹⁰. Unnikrishnan *et al.*¹¹ and Sundar and Shetye¹² have referred to the tidal constituents along the west coast of India. However, no information is available on the M₂ tidal constituent. Characteristics of tides in KB remain largely unknown. The present measurements are targeted to fill the gap that exists till date. Thermohaline features of KB and its sensitivity to meteorological influences have been reported by Joseph *et al.*¹³.

Data collection and analysis

Tidal measurements at KB

In KB, tidal data have been collected from eight stations. Whereas data from Kochi inlet of KB (see Figure 1) were obtained from a conventional float-driven gauge (paper

chart) maintained by the Survey of India, those from the other seven locations in KB have been collected at 10-min interval using EMCON-make float-driven electronic tide gauges during April–June 2006. Data collection from KB was carried out as part of a programme on Ecosystem Modeling of the Kochi Backwaters. In contrast to the bulky float-driven gauges, which are conventionally used in several harbours world over, the EMCON gauge incorporated a miniature stilling-well in the gauge design to suit this shallow estuary. The submerged portion of the stilling-well was provided with arrays of circular perforations, which function as low-pass hydraulic filter and serves good mixing with external waters^{14,15} and also minimizes the Bernoulli dynamic pressure effects^{16,17}. With these modifications, the stilling-wells used in the present measurements were free from most of the inadequacies inherent with the conventional stilling-wells (e.g. refs 15 and 18–24).

Tidal constituents

Tide is the all-weather rising and lowering of water level, produced by a combination of varying astronomical forces and earth's rotation; and is considered to be one of the most regular and rhythmic motions in nature. As the astronomical setting of a given location on earth relative to sun and moon is rather complex, similar complexities are present in the tidal oscillations as well. Although tides have an astronomical origin, the response of a given location to the tidal forces is influenced considerably by a myriad of complex topographical influences (varying depths, boundaries, resonance, etc.). The so-called shallow-water constituents resulting from such influences can be distinguished in over-tides and compound-tides, which represent the nonlinear harmonics that are generated in areas of large bottom friction such as in coastal waters, estuaries and semi-enclosed water bodies such as backwater systems. The over-tides have an angular speed, which is an exact multiple of the angular speed of one of the astronomical constituents. However, the angular

speed of a compound-tide equals the sum or the difference of the angular speeds of two or more astronomical constituents. Thus, the tidal oscillation at a place can be represented by a sum of astronomical constituents and its over-tides and compound-tides. Therefore, a Fourier description (i.e. various cosine series of partial tides) really

well represents the features of tidal motion at a place. The harmonic analysis of tidal observations consists essentially in the dissection of the aggregate tidal oscillations into a number of partial constituent waves. The tidal constituents obtained from harmonic analysis of an adequately long (usually 1 year) previously known time-series records of the tidal measurements at a given location represent the purely astronomical as well as the topographically induced influences on the tidal motion experienced at that location. From this, it is possible to determine the amplitude and phase (known as ‘tidal constants’) of each tidal constituent (i.e. partial tide). These constants remain unaltered as long as the geometry of the water body and the bed materials that contribute to the bottom friction remain unaltered. The only constituents that are not obtained as a consequence of limiting the tidal measurements to one month are those with periods of $\frac{1}{2}$ year (solar semi-annual constituent, S_{sa}) and 1 year (solar annual constituent, S_a). In any case, the amplitudes of these two constituents are considerably smaller than those of the major tidal constituents. Prediction of tidal oscillation for a given location involves a process of synthesis by summing up an adequate number of harmonic constituents (i.e. various cosine series of partial tides), of different amplitudes and phases, for that location.

Tidal measurements reported here have been acquired at fast sampling interval (10 min), and are free from gaps. Because of fast sampling, the tidal curves (represented by a finite number of harmonic constituents) are well represented. However, water level oscillations in KB are influenced by a myriad of surface-meteorological and hydrological factors (substantial amount of freshwater influx from a network of rivers) in addition to the well-known astronomical forcing²⁵ and, therefore, considerable amount of non-tidal contributions were present in the measurements. Following conventional practice, the data was smoothed (by applying a three-point moving-average filter to the respective time-series) and the non-tidal contribution (i.e. residual) was removed from the measured data using known techniques of tidal analysis.

Tidal constituents (i.e. amplitude and phase) were determined by the method of least-squares. In this, the fitting is adjusted so that the square, of the difference between the observed and computed tidal levels when summed over all the observed values, has its minimum value. The least-squares-fitting is performed by computer matrix inversion. For this analysis, we used a Tidal Analysis Software Kit (TASK), developed at the Proudman Oceanographic Laboratory, UK²⁶. The TASK-2000 package originated from a set of programs for tidal analysis derived primarily from the TIRA tidal analysis programs²⁷. This scheme resolved 25 tidal constituents which describe the salient features of the astronomical tides for each station in KB. The tidal constituents derived from the measurements at eight stations in KB are summarized in Table 2. These constants remain invariant

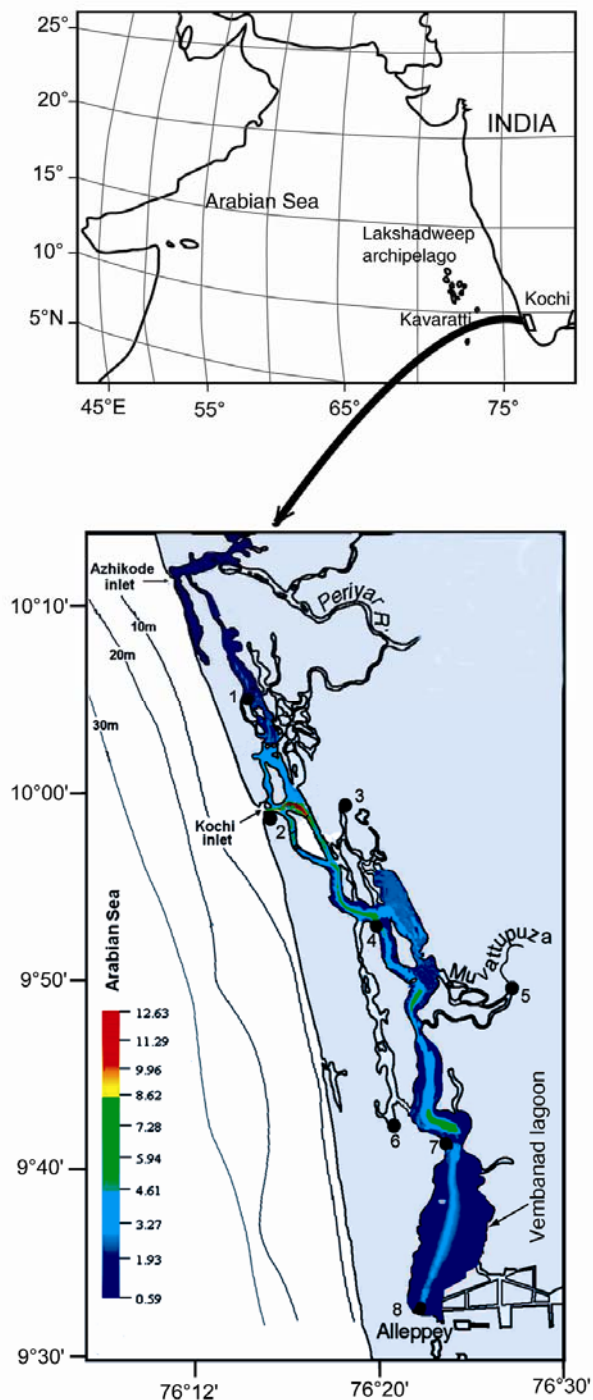


Figure 1. Location map of tidal measurements at eight stations in Kochi backwaters on the southwest coast of India. Closed circles show the measurement locations and the associated number is the station number. Graph legend in the bottom figure panel represents depth.

Table 2. Summary of tidal constituents from station nos 1–8 of Kochi backwaters on the southwest coast of India. Station numbers correspond to those indicated on the location map in Figure 1. H and G represent the amplitude (cm) and phase (°) respectively of the tidal constituent

Tidal constituent	Station numbers (Kochi backwaters on the southwest coast of India)															
	1		2		3		4		5		6		7		8	
	H	G	H	G	H	G	H	G	H	G	H	G	H	G	H	G
M ₂	18.0	26.6	21.5	338.8	13.7	31.5	12.2	20.8	7.9	67.1	9.0	80.0	7.3	90.3	7.0	124.8
K ₁	13.8	90.5	18.1	61.0	10.9	100.5	10.9	96.1	7.4	123.2	8.7	125.9	8.3	128.3	7.2	142.6
O ₁	6.5	75.3	8.7	58.2	5.0	79.1	4.7	76.0	3.9	98.4	4.1	101.4	3.7	104.4	3.2	108.1
S ₂	5.7	97.7	9.2	36.3	4.1	96.5	3.8	82.9	2.3	134.3	2.8	142.6	2.1	153.2	1.7	206.7
N ₂	2.9	0.9	5.6	299.6	2.3	352.8	2.3	343.5	1.7	33.2	1.1	32.1	1.1	46.1	0.9	71.4
MK ₃	1.8	25.6	0.4	159.9	0.9	63.5	0.8	62.2	0.9	74.6	0.8	112.5	0.4	158.5	1.0	199.7
MU ₂	1.5	91.8	1.1	143.2	0.6	137.6	0.4	119.6	0.4	239.5	0.6	190.1	0.4	216.4	0.5	217.5
Q ₁	1.1	106.3	1.8	35.9	0.7	77.1	0.8	74.1	0.4	66.2	0.5	121.1	0.2	117.5	0.3	178.9
MO ₃	1.1	106.3	0.1	197.5	0.5	160.8	0.7	151.3	0.0	290.9	0.7	227.3	0.5	248.5	0.5	273.0
L ₂	0.8	98.1	1.8	198.0	0.2	54.0	0.3	118.1	0.3	327.1	0.3	87.2	0.3	221.1	0.6	180.9
J ₁	0.7	130.9	0.6	72.2	0.7	175.9	0.4	140.4	0.6	182.3	0.3	210.8	0.2	267.9	0.2	147.9
M ₆	0.5	166.1	0.1	82.0	0.1	199.9	0.3	227.0	0.3	342.9	0.2	11.4	0.2	350.5	0.1	191.2
OO ₁	0.5	45.3	0.9	137.1	0.3	79.3	0.5	94.7	0.5	138.2	0.4	101.1	0.6	121.1	0.7	141.0
M ₁	0.5	106.0	1.0	43.8	0.5	129.4	0.4	123.8	0.3	100.7	0.2	137.0	0.2	140.4	0.3	240.2
2SM ₂	0.4	302.9	0.9	177.1	0.5	288.7	0.3	297.9	0.2	268.8	0.2	24.9	0.2	63.4	0.3	76.5
SN ₄	0.4	307.2	0.2	49.3	0.1	28.1	0.3	22.5	0.2	50.7	0.3	63.4	0.1	90.2	0.3	155.2
MN ₄	0.3	285.1	0.5	9.6	0.1	306.1	0.2	277.5	0.3	345.4	0.2	43.0	0.1	120.9	0.3	140.4
M ₃	0.2	133.0	0.4	229.8	0.2	144.2	0.3	137.2	0.0	104.1	0.2	158.7	0.1	187.5	0.3	237.3
MSN ₆	0.2	199.3	0.2	108.4	0.1	241.0	0.2	252.2	0.2	23.3	0.1	27.2	0.1	300.0	0.2	167.6
2MS ₆	0.1	216.7	0.4	195.5	0.2	268.1	0.5	308.8	0.4	59.3	0.4	69.3	0.2	27.1	0.2	186.8
2SM ₆	0.1	339.8	0.1	252.5	0.1	306.9	0.1	32.3	0.2	130.7	0.1	124.7	0.1	51.9	0.2	194.4
2MN ₆	0.1	96.1	0.1	72.2	0.0	180.3	0.1	187.0	0.1	313.3	0.1	297.2	0.1	55.5	0.1	143.3
Msf	6.7	348.1	3.5	295.3	3.7	351.9	4.6	356.5	4.5	353.8	6.5	342.0	6.5	342.3	9.6	28.0
M ₄	0.7	288.1	0.5	108.4	0.8	293.0	0.8	293.6	0.8	6.5	0.8	18.8	0.4	16.8	0.4	116.2
MS ₄	0.6	325.0	0.5	170.6	1.0	26.3	1.0	17.0	1.1	85.5	1.0	86.5	0.6	80.9	0.7	165.7

as long as the geological setting (i.e. bathymetry, topography, bed materials, etc.) of a sufficiently large region in the vicinity of the given location, remains unchanged. The predicted tides (i.e. water level oscillations free from meteorological and hydrological influences) from eight spatially distributed stations covering most of the segments of KB are shown in Figure 2.

Results

The tidal patterns from eight locations presented in Figure 2 provide a glimpse of the transformation undergone by the tide during its propagation from the dual-mouth region of KB to its shallow upstream boundary. The prominent features that are readily seen in the tidal patterns include, first, a rather progressive attenuation of tidal range from its major mouth (Kochi inlet) up to the upstream boundary (Figure 3a) and corresponding attenuation of the amplitude of the five major tidal constituents M₂, K₁, O₁, S₂ and N₂ (Figure 3b). Second, the daily-mean of the astronomical tides (thick central lines in Figure 2) from several stations in the study areas are modulated by oscillations of fortnightly periodicity; this feature being most dominant at station #8 in the Vembanad Lake, located close to the upstream (i.e. southern-

most) region of KB, and a second station located approximately midway between the dual-mouths of KB (i.e. station #1).

Amongst all the tidal constituents obtained from tidal analysis (Table 2), the only constituent having fortnightly periodicity is Msf. The relative importance of Msf tidal constituent amongst other constituents in the present study is its selective amplification in the upstream direction of KB (Figure 3c) where the major constituents get attenuated ~73% relative to those at the mouth (Figure 3b).

Discussion

Msf equilibrium tide

One of the reasons for the development of Msf tide is the response of the water body to the driving tidal potential^{2,28–30}, based on which the amplitude of the Msf equilibrium tidal constituent is given by the expression:

$$A_{\text{Msf}} = [0.123(1-3 \sin^2\Phi) \cos(2s-2h)], \quad (1)$$

where Φ is the geographical latitude and $(2s-2h)$ the angular speed of Msf tide in degree per solar hour. In this,

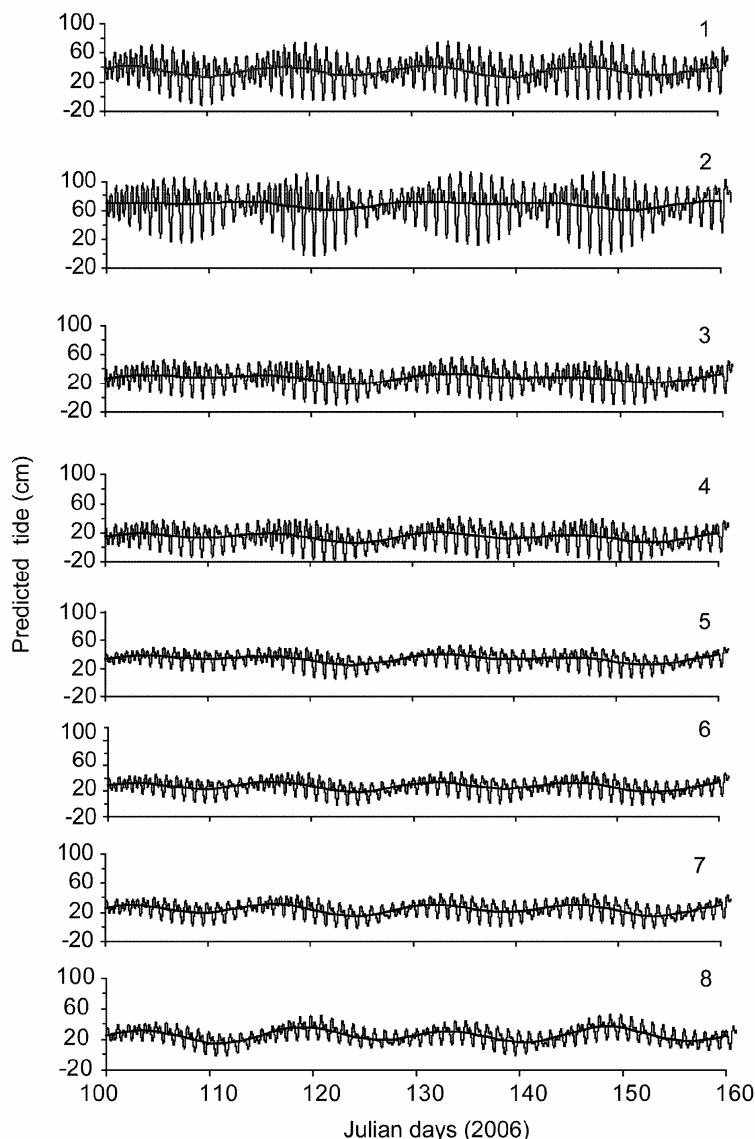


Figure 2. Predicted tides (i.e. water level oscillations free from meteorological and hydrological influences) covering eight stations in Kochi backwaters on the southwest coast of India. The central line through the tidal curve represents the 1-day (144-point) moving average values of the tide. Numbers 1–8 on the top right-hand side of the tidal pattern are station numbers indicated in Figure 1.

the parameters s and h are the positions of the moon and sun in the sky (the ‘mean longitudes’). In a lunar month and a solar year, s and h respectively goes through 0° to 360° . Consequently $(2s - 2h)$ goes through 0° to 360° in 14.76 days, i.e. $1.0159^\circ/\text{solar hour}$. Based on the estimate using the above formula, the amplitude of the Msf equilibrium tide in the present study region is <2 mm, which is too small relative to the observed amplitudes.

Resonance

Selective amplification of certain tidal constituents is often observed in various water bodies, including continental

shelves and estuaries. Amplification of semi-diurnal tides in the Gulf of Kutch and Gulf of Khambhat on the northwest coast of India arising partly from quarter wavelength resonance^{11,31,32} is an example of selective amplification of tidal constituents. Msf tidal amplification by quarter wavelength resonance in a semi-enclosed estuary such as KB requires that its average length L and average depth D must relate to the time-period T of the oscillation (in the present case, Msf tidal constituent) through a mathematical expression given by:

$$T = \frac{4L}{\sqrt{gD}}, \tag{2}$$

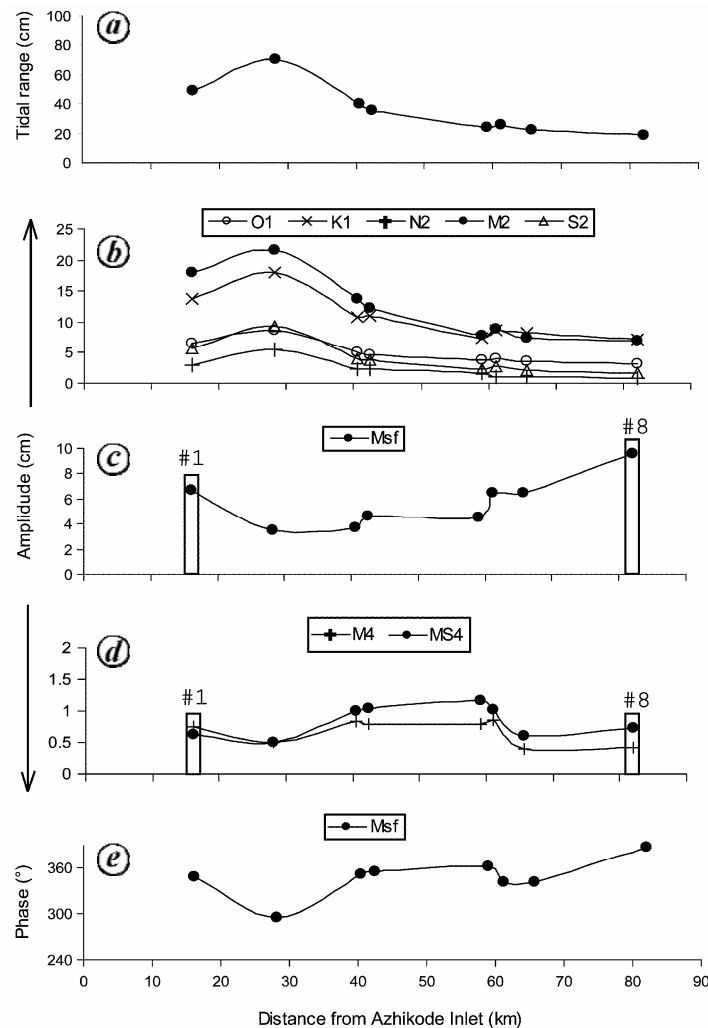


Figure 3. Characteristics of tides at eight stations in Kochi backwaters on the southwest coast of India. (a) Tidal range; (b) Amplitudes of 5 major tidal constituents; (c) Amplitudes of Msf tides; (d) Amplitudes of M_4 and MS_4 tides; (e) Phases of Msf tides.

where g is the gravitational acceleration. The average depth of KB being 2.50 m, the length required to amplify Msf tide ($T = 14.76$ days) by this mechanism is 1579 km. However, the length of KB (~82 km) is too short to develop the required resonance condition. Therefore, the observed amplification of Msf tidal constituent at KB is not a consequence of quarter-wavelength resonance.

Nonlinear bottom-frictional interaction between M_2 and S_2 tides

Tidal oscillation at a given location contains contributions from a myriad of astronomical forces governed by a complicated non-linear celestial dynamical system, and is further modified by several topographically induced influences. Mutual interaction of certain tidal constituents in estuaries and backwater systems can play an important influence on the propagation and shape of the tide wave.

We examine a known mechanism, namely a nonlinear bottom-frictional interaction between the M_2 and S_2 tidal constituents for the development and amplification of Msf tide at several locations in the present study area. In shallow water, nonlinear frictional interaction between M_2 and S_2 tides can generate Msf tide with amplitude considerably larger than that in eq. (1). When shallow-water effects are proportional to the square of the tidal water level through a spring-neap cycle, four harmonic constituents can be generated, as given by³³:

$$\begin{aligned}
 & K \{ (H_{M_2} \cos(2\omega_1 t) + H_{S_2} \cos(2\omega_0 t))^2 \\
 & = K \left\{ \frac{1}{2} (H_{M_2}^2 + H_{S_2}^2) + \frac{1}{2} H_{M_2}^2 \cos(4\omega_1 t) \right. \\
 & \quad + \frac{1}{2} H_{S_2}^2 \cos(4\omega_0 t) + H_{M_2} H_{S_2} \cos 2(\omega_1 + \omega_0) t \\
 & \quad \left. + H_{M_2} H_{S_2} \cos 2(\omega_0 - \omega_1) t \right\},
 \end{aligned}$$

where K is a constant whose value depends on the topographic and geomorphologic properties of the area, H the tidal water level, and ω_1 and ω_0 are the lunar and solar harmonic angular speeds (radians) respectively and t the time. The mutual interaction has produced a change in the mean water level, represented by a long-period harmonic variation with a speed equal to the difference in the speeds of the interacting constituents, $2(\omega_0 - \omega_1)$, called Msf constituent. Thus, the Msf harmonic constituent is expressed as $(K \times H_{M_2} H_{S_2} \cos 2(\omega_0 - \omega_1)t)$ in which H_{M_2} and H_{S_2} are the heights of the M_2 and S_2 tides respectively. With $\omega = 2(\omega_0 - \omega_1)$,

$$\frac{1}{T} = 2 \left(\frac{1}{T_0} - \frac{1}{T_1} \right)$$

where T , T_0 and T_1 are the time-periods corresponding to ω , ω_0 and ω_1 respectively. If periods are expressed in terms of mean solar day, then $T_0 = 1$ and $T_1 = 1.0351$ (ref. 33), so that $T = 14.76$ solar days. The Msf tidal period estimated as above is the same as the period of the spring-neap modulations on the tidal amplitudes. Thus, the Msf tidal constituent generated by this nonlinear bottom-frictional interaction mechanism represents the changes in mean water level over a spring-neap cycle due to M_2 acting on S_2 or vice-versa, often referred to as tidal pumping in tidal theory^{7,34}. Two other harmonic constituents observed in the present study areas as a result of this nonlinear frictional interaction effect are the fourth-diurnal species M_4 (over-tide) with angular speed $4\omega_1$ (expressed as $(K/2) \times (H_{M_2})^2 \cos 4\omega_1 t$) and MS_4 (compound tide) with angular speed $2(\omega_1 + \omega_0)$ (expressed as $K \times H_{M_2} H_{S_2} \cos 2(\omega_1 + \omega_0)t$). However, S_4 harmonic constituent (with angular speed $4\omega_0$) is absent in KB.

Figures 3 *c* and *d* show that, as expected from the nonlinear frictional interaction theory addressed above, the changes in amplitudes of Msf, M_4 and MS_4 follow similar trend in general, in which the Msf amplitude is about 4–16 times larger than the corresponding M_4 and MS_4 amplitudes at several locations in KB. However, the observed amplitudes of Msf tide in two specific regions (bounded within vertical columns in Figure 3 *c*), namely; (i) a station located approximately midway between the dual-mouths of KB (station #1), and (ii) the uppermost (i.e., southernmost) station in KB [station #8], are considerably larger than what is inferred from the amplitudes of the corresponding M_4 and MS_4 constituents in the other stations of the present study area. For example, at station #1, the Msf amplitude is ~10 and 11 times larger than the amplitudes of the corresponding M_4 and MS_4 tides respectively. At station #8, the Msf amplitude is ~24 and 14 times larger than the amplitudes of the corresponding M_4 and MS_4 tides respectively. This indicates that whereas nonlinear frictional interaction between M_2 and S_2 tides is primarily responsible for the amplification

of Msf tidal constituent at most stations of the study area, the two specific regions mentioned above (stations #1 and #8) possess some peculiarities which distinguish them clearly from the other regions.

Variable bottom friction

As indicated in the above discussion, two specific regions in the study area where the amplitude of the Msf tide distinctly stands out in relation to those in the neighbourhood regions are – a station located approximately midway between the dual-mouths of KB (station #1), and the southernmost station in KB (station #8). In these locations, the Msf amplitude (Figure 3 *c*) in relation to that of the corresponding M_4 and MS_4 constituents (Figure 3 *d*) is considerably larger than those observed in other locations.

Shallowness: While examining the geographical features of these two regions in an attempt to derive some clues regarding the observed enhancement of Msf tidal amplitudes there, an important factor that stands out clearly is the considerably shallower bathymetry of these regions relative to the rest of the regions in the study area. For example, station #1 is the delta of six rivers including River Periyar and is considerably shallow (~2 m). Generation of large amplitude Msf tide has been reported from other shallow deltaic regions as well. For example, considerably large Msf amplitude (~25 cm) was reported at Forcados of the Niger River Delta on the northeast corner of the Gulf of Guinea³⁵. The Vembanad Lake, which is the southern extension of KB (~20 km in the upstream direction and having an area of ~70 km²) and encompassing station #8 is also considerably shallow (<2 m). Thus, a striking similarity among the two stations, where enhanced Msf tidal amplification exists, is their relatively shallow depths.

As a result of considerable shallowness (relative to the chart datum level) of these two regions, the water level above the bed undergoes relatively large changes between spring and neap tides. Although the driving force for tidal currents acts uniformly through the water column, the bottom friction arising from considerable shallowness reduces tidal currents at the bottom. Tidal currents are sensitive to changes of depth, showing a vertical structure near the bed³⁶. Considerable reduction in bottom currents relative to those at the upper layers of the water column gives rise to an increase of ‘mean-level’ due to ‘set-up’³³. Tidal currents are maxima during spring tides and therefore, the vertical gradient of the horizontal currents is also maxima during this phase of the tide, with maximum horizontal current at the topmost layer and the minimum horizontal current at the bottom layer. Thus, the set-up is a maximum during spring tide. The reverse happens during neap tide, when tidal currents are weak and therefore, the horizontal current stratification in the vertical direc-

tion is also weak. Hence, the mean set-up varies over the spring-neap cycle, giving rise to friction-induced build up of Msf tide at the two regions mentioned above. A variation of 'mean-level' over a 14-day spring-neap cycle, as described above, is clearly seen in the KB, especially the southern regions (Figure 2). A similar effect was observed in the Amazon estuary⁵ and in the Fleet, an English tidal lagoon in which the Msf tide is an order of magnitude larger than other tidal constituents⁴. The observed Msf tidal amplification in the southernmost region of KB is ~3-fold. Based on the arguments put forward above in terms of shallowness of seabed and the influence of tidal current stratification in the development of a water level setup in considerably shallow water bodies, it is inferred that the relatively large Msf tidal amplitude observed in two specific regions in the present study areas (stations #1 and #8) stems primarily from variable bottom frictional effects at fortnightly periodicity arising from the relatively lesser depth of the bed. However, the presence of M_4 and MS_4 tidal constituents in all the above two regions suggests that frictional interaction between M_2 and S_2 tides also contributes to the generation and amplification of Msf tides there. Thus, combined effects of a nonlinear frictional interaction mechanism operating between M_2 and S_2 tides and spring-neap variability in bottom-friction together contribute to the development of significantly large Msf tide observed in the above two regions in the present study area.

Bed materials: In the context of the role of bottom-friction in the generation and amplification of Msf tidal constituent, it would be appropriate to examine the geomorphologic nature of the floor (nature of bed materials) in those two regions of the present study area which give rise to considerable amplification of Msf tidal constituent relative to the corresponding M_4 and MS_4 tidal amplitude. Station #1 in the present study area is a river delta in which the bed materials are composed of fine clay³⁷. On the other hand, the bed materials in the region encompassing station #8 are of sandy nature³⁸. Amongst the above bed materials, fine clay offers the least bed-roughness³⁹. Thus, amongst the two stations (#1 and #8) under consideration, the deltaic region located between the two mouths of KB (station #1) and Vembanad Lake (station #8) offers respectively the least and the most bed-roughness. It is seen that station #8, which exhibits the largest bed friction, generates the largest Msf amplitude relative to the corresponding M_4 and MS_4 tidal amplitude.

Conclusions

Characteristics of tides at eight locations in the KB on the southwest coast of India have been examined. Tidal constituent analysis shows that amplitudes of the fortnightly Msf tidal constituent at several locations in KB are con-

siderably larger than those estimated from the driving tidal potential. In KB, the amplitude of the Msf constituent amplifies progressively from its major mouth (~3-fold amplification in a shallow region at the upstream boundary), whereas the five major constituents M_2 , K_1 , O_1 , S_2 and N_2 attenuate progressively from the mouth (~73% attenuation at the upstream boundary region). Based on the observed large amplitudes of the Msf tide, over-tide M_4 , and compound tide MS_4 , it is found that the amplification of Msf tide observed at most of the stations in KB is attributable to non-linear frictional interaction between M_2 and S_2 tides. However, the relatively much larger Msf tide observed at a station located approximately midway between the two mouths of KB (~7 cm), and at the upstream boundary of this backwater system (~10 cm, which is ~3-fold larger than at the mouth) are attributable to an additional contribution from variable bottom frictional effects at fortnightly periodicity, arising primarily from shallowness of bed (<2 m) and bed material.

Our study indicates that shallow and broad estuarine water bodies are probable sites for large Msf tides. The large Msf tides observed at some locations in KB may have environmental implications in terms of variable flushing at fortnightly periodicity, with the possibility of larger flushing during the crust phase of the Msf tide.

1. Wunsch, C., The long-period tides. *Rev. Geophys.*, 1967, **5**, 447–476.
2. Picaut, J. and Verstraete, J. M., Propagation of a 14.7-day wave along the northern coast of the Guinea gulf. *J. Phys. Oceanogr.*, 1979, **9**, 136–149.
3. Le Blond, P. H., Forced fortnightly tides in shallow rivers. *Atmosphere–Ocean*, 1979, **17**, 253–264.
4. Robinson, I. S., Warren, L. and Longbottom, J. F., Sea-level fluctuations in the Fleet, an English tidal estuary. *Estuarine Coastal Shelf Sci.*, 1983, **16**, 651–668.
5. Gallo, M. N. and Vinzon, S. B., Generation of over-tides and compound tides in Amazon estuary. *J. Ocean Dyn.*, 2005.
6. Manoj, N. T., Unnikrishnan, A. S. and Sundar, D., Tidal asymmetry in the Mandovi and Zuari estuaries, the west coast of India. *J. Coastal Res.*, 2009, **25**, doi: 10.2112/08-1056.1 (in press).
7. Woodworth, P. L., Blackman, D. L., Pugh, D. T. and Vassie, J. M., On the role of diurnal tides in contributing to asymmetries in tidal probability distribution functions in areas of predominantly semi-diurnal tide. *Estuarine Coastal Shelf Sci.*, 2005, **64**, 235–240.
8. Wunsch, C., Haidvogel, D. B., Iskandarani, M. and Hughes, R., Dynamics of the long-period tides. *Prog. Oceanogr.*, 1997, **40**, 81–108.
9. Srinivas, K., Revichandran, C., Maheswaran, P. A., Asharaf, T. T. M. and Murukesh, N., Propagation of tides in the Cochin estuarine system, southwest coast of India. *Indian J. Mar. Sci.*, 2003, **32**, 14–24.
10. Balachandran, K. K., Reddy, G. S., Revichandran, C., Srinivas, K., Vijayan, P. R. and Thottam, T. J., Modelling of tidal hydrodynamics for a tropical ecosystem with implications for pollutant dispersion (Cochin estuary, southwest India). *Ocean Dyn.*, 2008, **58**, 259–273.
11. Unnikrishnan, A. S., Gouveia, A. D. and Vethamony, P., Tidal regime in Gulf of Kutch, west coast of India, by 2D model. *J. Waterway Port Coast. Ocean Eng.*, 1999, **125**, 276–284.

12. Sundar, D. and Shetye, S. R., Tides in the Mandovi and Zuari estuaries, Goa, west coast of India. *J. Earth Syst. Sci.*, 2005, **114**, 493–503.
13. Joseph, A. *et al.*, Observed thermohaline structure and cooling of Kochi backwaters and adjoining southeastern Arabian Sea. *Curr. Sci.*, 2009, **96**, 364–375.
14. Joseph, A., Vijaykumar, K., Desa, E. S., Desa, E. and Peshwe, V. B., A technique to circumvent lower density water trapping by tide-wells, Proceedings of the National Symposium on Ocean Electronics – SYMPOL'99, Cochin University of Science and Technology, 1999, pp. 55–63.
15. Joseph, A., Vijaykumar, K., Desa, E. S., Desa, E. and Peshwe, V. B., Over-estimation of sea level measurements arising from water density anomalies within tide-wells – a case study at Zuari Estuary, Goa. *J. Coastal Res.*, 2002, **18**, 362–371.
16. Joseph, A., Foden, P. and Taylor, K., An experimental evaluation of flow-induced errors in a pressure transducer and some design solutions to improve its performance in a flow-field, Internal Document No. 82, Proudman Oceanographic Laboratory, 1995, p. 52.
17. Joseph, A., Desa, J. A. E., Foden, P., Taylor, K., McKeown, J. and Desa, E., Evaluation and performance enhancement of a pressure transducer under flows, waves, and a combination of flows and waves. *J. Atmos. Oceanic Technol.*, 2000, **17**, 357–365.
18. Cross, R. H., Tide gage frequency response. *J. Waterways Harbor Div. Proc. Am. Soc. Civil Eng.*, 1968, **94**, 317–330.
19. Noye, B. J., Tide-well systems I: Some non-linear effects of the conventional tide-well. *J. Mar. Res.*, 1974, **32**, 129–153.
20. Braddock, R. D., Response of a conventional tide gauge to a tsunami. *Mar. Geodesy*, 1980, **4**, 223–236.
21. Shih, H. H. and Porter, D. L., Error models for stilling-well – Float type tide gauges, Proceedings of IEEE Oceans'81, 1981, pp. 1118–1123.
22. Loomis, H. G., The non-linear response of a tide gauge to a tsunami. Proceedings of the 1983 Tsunami Symposium, 1983, pp. 177–185.
23. Satake, K., Okada, M. and Abe, K., Tide gauge response to tsunamis: Measurements at 40 tide gauge stations in Japan. *J. Mar. Res.*, 1988, **46**, 557–571.
24. Shih, H. H. and Baer, L., Some errors in tide measurement caused by dynamic environment. In *Tidal Hydrodynamics* (ed. Parker, B. B.), John Wiley, New York, 1991, pp. 641–671.
25. Joseph, A. *et al.*, Vulnerability of Cochin backwaters to meteorological disturbances with special reference to tidal propagation, Proceedings of the National Symposium on Emerging Trends in Meteorology and Oceanography, 2007 (eds Vijayakumar, D. *et al.*), METOC-2007, School of Naval Oceanology and Meteorology, Kochi, 21–22 May 2007, pp. 67–76.
26. Bell, C., Vassie, J. M. and Woodworth, P. L., POL/PSMSL Tidal Analysis Software Kit 2000 (TASK-2000), Permanent Service for Mean Sea Level, Proudman Oceanographic Laboratory, UK, 2000.
27. Murray, M. T., A general method for the analysis of hourly heights of the tide. *Int. Hydrogr. Rev.*, 1964, **41**, 91–101.
28. Doodson, A. T. and Warburg, H. D., *Admiralty Manual of Tides*, London, HMSO, 1941, p. 270.
29. Cartwright, D. E. and Taylor, R. J., New computations of the tide generating potential. *Geophys. J. R. Astron. Soc.*, 1971, **23**, 45–74.
30. Cartwright, D. E. and Edden, A. C., Corrected tables of tidal harmonics. *Geophys. J. R. Astron. Soc.*, 1973, **33**, 253–264.
31. Shetye, S. R., Tides in the Gulf of Kutch, India. *Continental Shelf Res.*, 1999, **19**, 1771–1782.
32. Nayak, R. K. and Shetye, S. R., Tides in the Gulf of Khambhat, west coast of India. *Estuarine Coastal and Shelf Sci.*, 2003, **57**, 249–254.
33. Pugh, D. T., *Tides, Surges and Mean Sea-Level*, A Handbook for Engineers and Scientists, John Wiley, 1987, p. 472.
34. Woodworth, Proudman Oceanographic Laboratory, Pers. Commun., 2007.
35. Clarke, A. J. and Battisti, D. S., Identification of the fortnightly wave observed along the northern coast of the Gulf of Guinea. *J. Phys. Oceanogr.*, 1983, **13**, 2192–2200.
36. Howarth, M. J., Tidal currents of the continental shelf. In *Offshore Tidal Sands* (ed. Stride, A. H.), Chapman & Hall, London, 1982, p. 222.
37. Ramamirtham, C. P. and Muthusamy, S., Estuarine oceanography of the Vembanad Lake – Part II: the region between Cochin and Azhikode. *Indian J. Fisheries*, 1986, **33**, 218–224.
38. Josanto, V., On the grain size distribution of the Cochin backwater sediments. *Bull. Dept. Mar. Biol. Oceanogr.*, 1971, **5**, 109–122.
39. Chakraborty, B. and Pathak, D., Sea-bottom backscatter studies in the western continental shelf of India. *J. Sound Vibr.*, 1999, **219**, 51–62.

ACKNOWLEDGEMENTS. Tidal observations from Kochi backwater system were made as part of a project on Integrated Coastal and Marine Area Management (ICMAM). This research has been supported in part by ICMAM (Ministry of Earth Sciences, Chennai) and the Council of Scientific and Industrial Research (CSIR), New Delhi. Tidal data from Kochi inlet was provided by Marine Surveyor's Office, Cochin Port Trust. A.J. thanks Dr Philip Woodworth (Proudman Oceanographic Laboratory, UK) for useful discussions on Msf tide. Mr P. Pawaskar provided assistance for preparation of figures. This work is NIO contribution no. 4595.

Received 9 December 2008; revised accepted 29 July 2009